JBC Papers in Press. Published on May 21, 2018 as Manuscript RA118.001980
The latest version is at http://www.jbc.org/cgi/doi/10.1074/jbc.RA118.001980

Oxidative decarboxylation of pyruvate by 1-deoxy-D-xyulose 5-phosphate synthase, a central metabolic enzyme in bacteria

Alicia A. DeColli[1], Natasha S. Nemeria[2], Ananya Majumdar[3], Gary J. Gerfen[4], Frank Jordan[2], Caren L. Freel Meyers[1*]

[1]Department of Pharmacology and Molecular Sciences, The Johns Hopkins University School of Medicine, Baltimore, MD, 21205, United States
[2]Department of Chemistry, Rutgers University, Newark, NJ, 07102, United States
[3] Department of Chemistry, Johns Hopkins University, Baltimore, MD, 21218, United States
[4] Department of Physiology and Biophysics, Albert Einstein College of Medicine, Bronx, NY, 10461, United States

Running title: *O_2-dependent LThDP decarboxylation on DXP synthase*

[*]To whom correspondence should be addressed: C. Freel Meyers: Department of Pharmacology and Molecular Sciences, The Johns Hopkins University School of Medicine, Baltimore, MD, 21205, United States; cmeyers@jhmi.edu; Tel. (410) 502-4807; FAX. (410) 955-3023.

Keywords: DXP synthase, decarboxylase, oxygen binding, oxidation-reduction, redox, thiamine, enzyme mechanism, pyridoxal phosphate, oxygenase, oxidative decarboxylation

Abstract

The underexploited antibacterial target 1-deoxy-D-xyluose 5-phosphate (DXP) synthase, catalyzes the thiamin diphosphate (ThDP)-dependent formation of DXP from pyruvate and D-glyceraldehyde 3-phosphate (D-GAP). DXP is an essential intermediate in the biosynthesis of ThDP, pyridoxal phosphate, and isoprenoids in many pathogenic bacteria. DXP synthase catalyzes a distinct mechanism in ThDP decarboxylative enzymology in which the first enzyme-bound pre-decarboxylation intermediate, C2α-lactylThDP (LThDP), is stabilized by DXP synthase in the absence of D-GAP, and D-GAP then induces efficient LThDP decarboxylation. Despite the observed LThDP accumulation and lack of evidence for C2α-carbanion formation in the absence of D-GAP, CO_2 is released at appreciable levels under these conditions. Here, seeking to resolve these conflicting observations, we show that DXP synthase catalyzes the oxidative decarboxylation of pyruvate under conditions in which LThDP accumulates. O_2-dependent LThDP decarboxylation led to one-electron transfer from the C2α-carbanion/enamine to O_2, with intermediate ThDP-enamine radical formation, followed by peracetic acid formation *en route* to acetate. Thus, LThDP formation and decarboxylation and DXP formation were studied under anaerobic conditions. Our results support a model in which O_2-dependent LThDP decarboxylation and peracetic acid formation occur in the absence of D-GAP, decreasing the levels of pyruvate and O_2 in solution. The relative pyruvate and O_2 concentrations then dictate the extent of LThDP accumulation, and its buildup can be observed when [pyruvate] > [O_2]. The finding that O_2 acts as a structurally distinct trigger of LThDP decarboxylation supports the hypothesis that a mechanism involving small molecule-dependent LThDP decarboxylation equips DXP synthase for diverse, yet uncharacterized cellular functions.

Introduction

The increasing spread of antimicrobial resistance demands the development of novel antimicrobial agents. 1-deoxy-D-xyluose 5-phosphate (DXP) synthase is an underexploited antimicrobial target that catalyzes the formation of DXP from pyruvate and D-glyceraldehyde 3-phosphate (D-GAP, Figure 1) in many human pathogens (e.g. *Mycobacterium* and *Plasmodium falciparum*). DXP is an essential branch point metabolite that serves as a precursor in the biosynthesis of thiamin diphosphate (ThDP), pyridoxal phosphate, and indispensable isoprenoids in bacterial pathogens (Figure 1) (1-4). Given the widespread essentiality of DXP in pathogens and its absence in humans, selective

inhibition of DXP synthase could offer a new antimicrobial strategy (5-8).

DXP synthase possesses pyruvate decarboxylase and carboligase activity (Figure 1), reminiscent of other ThDP-dependent enzymes (9). However, its distinct structure (10-12) and unique random sequential, preferred order mechanism (13-17) distinguish DXP synthase from other enzymes in this class, including its closest mammalian homologs, transketolase and the E1 component of pyruvate dehydrogenase (10). In contrast to other ThDP-dependent enzymes that utilize classical ping-pong kinetics, DXP synthase stabilizes LThDP and requires ternary complex formation upon binding of D-GAP to trigger efficient decarboxylation of LThDP by an unknown mechanism (13, 15). These mechanistic insights have guided selective inhibitor design (5-8).

The requirement for ternary complex formation during catalysis was first proposed based upon $^{14}CO_2$ trapping studies demonstrating a low rate of CO_2 release in the absence of D-GAP (13). Circular dichroism (CD) and NMR studies subsequently revealed the accumulation of LThDP on DXP synthase in the absence of D-GAP, and provided evidence that D-GAP plays a role to induce efficient LThDP decarboxylation (15). These findings are consistent with a mechanism involving ternary complex formation on DXP synthase; however, these results do not explain the earlier observation that DXP synthase catalyzes multiple turnovers and CO_2 release in the presence of excess pyruvate. DXP synthase-dependent acetolactate formation was demonstrated (18), providing a possible explanation for the observed CO_2 release in the absence of D-GAP. However, the acetolactate synthase activity of DXP synthase was later shown to be exceedingly inefficient (15). LThDP stabilization on DXP synthase, coupled with inefficient acetolactate formation and a lack of evidence for C2α-carbanion generation in the absence of D-GAP (by detection of acetaldehyde formation from hydroxyethylThDP (HEThDP) or 2,6-dichlorophenolindophenol (DCPIP) reduction, Figure 2) (15) are collectively inconsistent with the extent of CO_2 release observed by Eubanks and Poulter (13). Given the unique requirement for a trigger of LThDP decarboxylation on DXP synthase, resolving this discrepancy is important.

Here, we report studies that reconcile these conflicting observations. Our results indicate that DXP synthase catalyzes oxidative decarboxylation of pyruvate by a mechanism involving O_2-dependent LThDP decarboxylation and subsequent oxidation of the C2α-carbanion to produce peracetic acid as an intermediate in acetate formation. Removal of O_2 does not significantly impact the rates of LThDP formation, D-GAP-dependent LThDP decarboxylation, or DXP formation suggesting O_2 does not influence the DXP-forming activity of DXP synthase. However, the stability of LThDP depends upon the presence or absence of O_2, indicating that mechanistic studies of LThDP formation and decarboxylation in the absence of D-GAP should be conducted under anaerobic conditions. This study provides key insights into our understanding of DXP synthase mechanism and raises interesting questions about the function of the unique requirement for ternary complex formation on DXP synthase.

Results

Product formation on DXP synthase in the absence of D-GAP

To obtain a comprehensive profile of products formed by the action of DXP synthase in the absence of D-GAP, the DXP synthase reaction using uniformly $^{13}C_3$-pyruvate was monitored over time by NMR. 1D ^{13}C (Figure 3) and 2D HCC-COSY experiments (Figure S1) experiments revealed enzyme-dependent depletion of pyruvate (resonances at δ 204.97 ppm (C1, dd), 170.13 ppm (C2, dd), 26.47 (C3, dd)) with concomitant formation of acetate (resonances at δ 181.41 ppm (C1, d) and 23.31 ppm (C2, d)) and bicarbonate (δ 160.36 ppm (s)) as the major products, indicating that CO_2 release occurs under conditions in which accumulation of LThDP is evident by CD analysis (Figures 3A-3C). Orthogonal biochemical assays were conducted to measure CO_2 release and pyruvate consumption. A $^{14}CO_2$ trapping assay was conducted as previously described (13), and showed DXP synthase and pyruvate-dependent $^{14}CO_2$ release over time, consistent with bicarbonate formation detected by NMR (Figure 3D). Concomitant with CO_2 release, DXP synthase-dependent pyruvate consumption was observed by the lactate dehydrogenase (LDH) assay (Figure 3E). Taken together, these results indicate that DXP synthase catalyzes the oxidative decarboxylation of pyruvate in the absence of D-

GAP. These findings are consistent with the evidence for CO_2 release reported by Eubanks and Poulter (13), yet puzzling in light of the CD evidence for LThDP accumulation and D-GAP-dependent LThDP decarboxylation on DXP synthase under these conditions (15). Thus, experiments were conducted toward understanding oxidative decarboxylation and determining the trigger for CO_2 release on DXP synthase under these conditions.

Oxidative decarboxylation of pyruvate proceeds via the ThDP-enamine radical and peracetic acid formation

Several routes were considered for DXP synthase-catalyzed acetate formation (Figure 4). These were based on previous reports of ThDP-dependent enzymes that catalyze the oxidative decarboxylation of pyruvate (19-21) and those that form radical ThDP intermediates (22-27). Following decarboxylation of LThDP, one-electron transfer from the C2α-carbanion/enamine **1** to molecular oxygen results in the formation of a C2-(α-hydroxy)-ethylideneThDP radical cation (ThDP-enamine radical) **2** and superoxide. In path A (Figure 4), recombination of **2** with superoxide would generate ThDP-bound peroxide intermediate **3**. Elimination of cofactor from **3** would yield peracetic acid which is susceptible to rapid chemical decomposition to acetate in HEPES, pH 8 (Figure S2) (20, 28). Elimination of H_2O_2 from **3** (path B, Figure 4) would afford acetylThDP **4**, which could undergo hydrolysis to release acetate and cofactor. Finally, in path C (Figure 4), a second electron transfer from **2** to superoxide could occur resulting in the production of H_2O_2 and **4** *en route* to acetate. Notably, only LThDP has been detected on DXP synthase by NMR following an acid quench, with no detectable formation of acetylThDP **4** (15, 16).

Each proposed pathway to acetate requires O_2 consumption and formation of a radical ThDP intermediate (**2**, Figure 4). To confirm that O_2 is utilized as a substrate by DXP synthase, the concentration of O_2 was monitored over time in the presence of varying concentrations of DXP synthase and pyruvate. Indeed, enzyme and pyruvate-dependent O_2 consumption was detected providing further support for DXP synthase-catalyzed oxidative decarboxylation of pyruvate (Figure 5, Table 1).

Electron paramagnetic resonance (EPR) studies of DXP synthase in the presence of unlabeled, $^{13}C_3$ and $^{2}H_3$ labeled pyruvate revealed the formation of a radical species at concentrations of approximately 1% of DXP synthase active centers (Figure 6, solid lines). The spectra generated with $^{2}H_3$-pyruvate (Figure 6A) displayed an observable narrowing with respect to the unlabeled sample (Figure 6B), as would be expected if the electron spin of the radical species experienced a decreased (albeit unresolved) hyperfine coupling to the deuterons derived from $^{2}H_3$-pyruvate relative to the protons of the unlabeled pyruvate. Moreover, spectra generated with $^{13}C_3$-pyruvate produced a spectrum (Figure 6C) with observable broadening with respect to the unlabeled sample, which is expected if the radical experienced the additional (unresolved) hyperfine coupling to the ^{13}C nuclei (nuclear spin ½) which is absent in the ^{12}C (nuclear spin = 0) sample.

The impact of the labeled pyruvate on the EPR spectrum of the radical species clearly implicates the contribution of carbon and hydrogen derived from pyruvate to the structure of the radical species. To determine if the EPR spectra are consistent with the ThDP-enamine radical species **2** (Figure 4), simulations were generated (Figure 6, dashed lines) using parameters (Table S1) previously determined for similarly structured radical species generated by other ThDP-dependent enzymes (22-26). All parameters were held constant in the three simulations, with the exception of the appropriate addition or scaling of hyperfine interactions for the labeled nuclei previously determined (22-26). The fits provide strong evidence that the radical intermediate generated by DXP synthase is consistent with 1-electron oxidation of the enzyme-bound C2α-carbanion intermediate **1** to form **2** *en route* to acetate.

To distinguish between paths A and B/C (Figure 4), we utilized two previously described biochemical assays that specifically monitor peracetic acid (path A) or H_2O_2 (paths B or C) formation (20, 29). DXP synthase-catalyzed peracetic acid formation was probed using a coupled assay with thionitrobenzoate (TNB, λ_{max} = 412 nm) which is readily oxidized by peracetic acid at a significantly higher rate (~3000-fold higher) compared to its oxidation by H_2O_2 (20), thus providing a selective detection method to

differentiate between peracetic acid and H_2O_2 production. Control experiments were conducted to confirm selective detection of peracetic acid under reaction conditions used here (Figure S3). Observation of DXP synthase-dependent oxidation of TNB (Table 1) suggests that peracetic acid is formed in the oxidative decarboxylation of pyruvate by DXP synthase. Further, the rate of DXP synthase-dependent peracetic acid formation is comparable to the rate of O_2 consumption under the same conditions (Table 1), suggesting that peracetic acid formation coincides with O_2 consumption, similar to acetolactate synthase and pyruvate decarboxylase (20). In an attempt to ascertain whether acetate formation occurs via either path B or C, we employed a discontinuous assay for selective detection of H_2O_2 (29). Unfortunately, control experiments conducted during this study indicate that H_2O_2 is unstable under these reaction conditions and, therefore, cannot be accurately detected by this method (Figure S4). Although DXP synthase-catalyzed H_2O_2 formation cannot be definitively ruled out, the comparable rates of TNB and O_2 consumption (Table 1) and lack of acetylThDP detection on DXP synthase to date support path A as the major route to acetate.

The newly revealed understanding that DXP synthase catalyzes the oxidative decarboxylation of pyruvate suggests a model (Figure 7) to explain the simultaneous observations of LThDP accumulation and CO_2 release in the absence of D-GAP. In the presence of O_2, LThDP decarboxylation occurs by an unknown mechanism, to form the C2α-carbanion which is then oxidized to form peracetic acid (Figure 7). This reaction cycle consumes pyruvate and O_2 and depletes a proportion of LThDP-bound DXP synthase; thus, the relative concentrations of O_2 and pyruvate dictate the extent to which LThDP accumulation and/or oxidative decarboxylation is observed. Over time, DXP synthase deoxygenates the solution to a point where LThDP decarboxylation no longer occurs efficiently, permitting stabilization of LThDP over a longer time scale. To provide support for this model, we conducted a series of experiments to determine the effect of O_2 on the activity of DXP synthase.

Characterization of triggers of CO_2 release on DXP synthase

To determine if O_2 acts as a trigger of CO_2 release, we conducted the CO_2 trapping and pyruvate consumption assays under anaerobic conditions, in the presence or absence of added O_2 (established by purging reaction mixtures in an environment of 90 % N_2/10 % H_2 mix). Under anaerobic conditions in the absence of D-GAP, CO_2 release and pyruvate consumption are significantly decreased (Figures 8A and 8B), suggesting O_2 is required for efficient release of CO_2 in the absence of D-GAP. The observed low levels of CO_2 release and pyruvate consumption under anaerobic conditions could result from incomplete removal of O_2 or slow acetolactate formation. Addition of O_2 to the anaerobic sample results in significant CO_2 release (Figure 8A), providing direct evidence for O_2-induced decarboxylation. Importantly, under anaerobic conditions, addition of a deoxygenated D-GAP solution results in significant CO_2 release which is consistent with our previous characterization of D-GAP as a trigger of efficient LThDP decarboxylation on DXP synthase (Figure 8A) (15).

Behavior of LThDP on DXP synthase under aerobic and anaerobic conditions

If the model depicted in Figure 7 is correct, the stabilization of LThDP on DXP synthase should be observed by CD under anaerobic conditions, and the LThDP species should be unstable in the presence of a trigger of CO_2 release (O_2 or D-GAP). As expected, addition of pyruvate to DXP synthase under anaerobic conditions leads to the emergence of a positive CD signal at 313 nm (Figure 9A) which has previously been characterized as LThDP on DXP synthase (15). The apparent $K_d^{pyruvate}$ under anaerobic conditions is 45 ± 2 μM (Table 2). As illustrated in Figure 9B, in the absence of added triggers, following saturation of DXP synthase with pyruvate, the LThDP signal is stable for > 4 h. Immediate depletion of the signal at 313 nm is observed upon addition of a deoxygenated solution of D-GAP (1000 μM, Figure 9C) or upon aeration of the sample (via opening the lid and mixing, Figure 9D), which further supports both D-GAP and O_2 as triggers of LThDP decarboxylation and is consistent with the model shown in Figure 7. Importantly, this suggests that under aerobic conditions, the reactive nature of the LThDP intermediate may lead to unreliable measurements

of $K_d^{pyruvate}$, depending upon the extent of O_2 introduction through mixing. Varied aeration will change the amount of pyruvate required for DXP synthase to effectively deoxygenate the solution and permit observation of significant LThDP accumulation. In contrast, pyruvate is not turned over when measurements are conducted in an anaerobic environment, permitting a more reliable measurement of the apparent $K_d^{pyruvate}$.

Steady state kinetic characterization of DXP formation under anaerobic conditions

DXP formation is the only known physiological function of DXP synthase, and our results indicate the possibility that O_2 may compete with D-GAP in the LThDP decarboxylation and/or carboligation steps leading to DXP formation. Thus, we investigated the steady-kinetics of DXP formation in the absence of O_2 to determine the effect of O_2 on the component steady state kinetic parameters, K_m and k_{cat}, of wild type *E. coli* DXP synthase. The results indicate that there is no significant difference in the kinetic parameters measured in the presence or absence of O_2 (Figure 10, Table 2).

Pre-steady state characterization of LThDP formation and decarboxylation under anaerobic conditions

Steady state CD analysis of LThDP accumulation on DXP synthase in the presence and absence of O_2 provides support for a model in which the stability of the LThDP signal depends on the level of O_2 in solution. This suggests that experiments measuring accumulation or depletion of LThDP may be confounded by O_2-dependent LThDP decarboxylation and pyruvate consumption under aerobic conditions. Therefore, the pre-steady state rates of LThDP formation and decarboxylation (in the presence of deoxygenated buffer, D-GAP, or O_2-saturated buffer) were determined to obtain more accurate measurements of these kinetic parameters. To determine the rate of LThDP formation on DXP synthase in the absence of O_2, DXP synthase in one syringe was rapidly mixed with pyruvate in the other syringe under anaerobic conditions. The results indicate a rate of 1.64 ± 0.21 s^{-1} for LThDP formation (k_1) on DXP synthase under anaerobic conditions that is comparable to the previously reported rate of LThDP formation under aerobic conditions (1.39 ± 0.05 s^{-1}) (15), showing O_2 does not significantly impact the kinetics of LThDP formation on DXP synthase (Figure 11, Table 3). It is interesting to note that under anaerobic conditions, following addition of pyruvate to the pre-formed DXP synthase-ThDP complex, there is a short lag phase (Figure 11, inset, region 1) followed by a decrease in the CD signal at 313 nm (Figure 11, inset, region 2) that immediately precedes the signal increase corresponding to LThDP formation (Figure 11, inset, region 3). This behavior of the CD signal was not observed under aerobic conditions (10), and could signify binding and/or conformational change(s) occurring on DXP synthase prior to LThDP formation in the absence of O_2.

A significant decrease in the CD_{313} signal upon the addition of a trigger to pre-formed LThDP is interpreted to coincide with LThDP decarboxylation (15). It follows that the CD signal corresponding to pre-formed LThDP should be minimally affected by the addition of deoxygenated buffer lacking O_2 or D-GAP triggers required for efficient LThDP decarboxylation. Consistent with this, a marginal change in the CD_{313} signal is observed upon rapid mixing of deoxygenated buffer in one syringe with pre-formed LThDP in a second syringe under anaerobic conditions (Figure 12A), in contrast to the significant decrease at 313 nm observed in the presence of D-GAP or O_2 (Figures 12B and 12C). The subtle change in CD signal detected in the absence of added trigger (Figure 12A) is likely due to incomplete removal of O_2 during the deoxygenation process, leading to decarboxylation of a small fraction of LThDP. While an accurate background rate of LThDP decarboxylation could not be determined in this case, apparent LThDP re-synthesis (k_{1r}) is suggested by the data (app $k_{1r} = 1.04 \pm 0.11$ s^{-1}). In contrast, the rates of LThDP decarboxylation (k_2) upon addition of O_2-saturated buffer or deoxygenated buffer containing D-GAP to preformed LThDP (prepared under anaerobic conditions) were 62.0 ± 8.9 s^{-1} and 50.3 ± 7.8 s^{-1}, respectively (Figures 12A-12C, Table 3), comparable to the rate of LThDP decarboxylation in the presence of D-GAP under aerobic conditions previously reported ($k_2 = 42 \pm 1$ s^{-1}) (15). These results suggest that LThDP decarboxylation occurs efficiently in the presence of either D-GAP or O_2. Notably, previously observed lag phases in the CD_{313} signal occurring immediately before and

after the sharp decrease in this signal corresponding to LThDP decarboxylation (16) are observed upon addition of D-GAP or O_2-saturated buffer to preformed LThDP generated under anaerobic conditions (Figures 12B and 12C, insets). These lag phases are proposed to signify conformational changes occurring prior to LThDP decarboxylation and immediately after LThDP decarboxylation prior to LThDP re-synthesis (16), a hypothesis that is supported by recent HDX-MS studies (12).

Discussion

Although important aspects of the DXP synthase mechanism are uncovered, gaps in our understanding of catalysis on this unique ThDP-dependent enzyme remain. The present study addresses a discrepancy in mechanistic studies of DXP synthase: the observation of slow CO_2 release in the absence of a known trigger LThDP decarboxylation, D-GAP (13), despite the accumulation of LThDP on the enzyme and lack of evidence for the post-decarboxylation intermediate (15). Our results reveal two roles of O_2: 1) as a distinct trigger of LThDP decarboxylation, and 2) as an acceptor substrate in the oxidation of the C2α-carbanion to form peracetic acid *en route* to acetate. Other ThDP-dependent enzymes are known to catalyze similar reactions (19-21, 30). However, due to the ability of DXP synthase to stabilize LThDP, and the lack of any indication that C2α-carbanion formation takes place in the absence of D-GAP, this oxygen-consuming reaction was not previously characterized. The results show that steady state and pre-steady state kinetic parameters are unchanged under anaerobic conditions suggesting O_2 does not affect catalytic steps prior to and including DXP formation. The apparent $K_d^{pyruvate}$ measured under anaerobic conditions is a more accurate estimation as anaerobic conditions prevent confounding reactions that occur in the presence of O_2 (i.e., depletion of pyruvate and LThDP). Although the oxygenase activity of DXP synthase does not appear to affect DXP-forming activity of wild type enzyme, this side reaction and discovery of O_2-dependent LThDP decarboxylation have important implications for the study of DXP synthase mechanism.

In retrospect, the observation of LThDP buildup on DXP synthase was fortuitous given the efficiency of decarboxylation in the presence of O_2, and points to the unique mechanistic aspects of this enzyme. The oxidative decarboxylation of pyruvate is a key element of DXP synthase mechanism that explains the accumulation of LThDP and lack of accumulation of the C2α-carbanion, despite significant CO_2 release (13, 15). Our inability to detect post-decarboxylation intermediates on DXP synthase in the absence of D-GAP, is likely a consequence of electron transfer from the C2α-carbanion to O_2 preventing efficient reaction of this intermediate with other potential acceptor substrates. The simultaneous observations of LThDP accumulation and CO_2 release can be explained by the model in Figure 7. Under conditions where O_2 is in excess to pyruvate, occurrence of LThDP decarboxylation at a lower rate than C2α-carbanion consumption, would permit the observation of the LThDP intermediate concomitant with CO_2 release and peracetic acid/acetate formation. The presence of O_2 ensures this cycle of LThDP decarboxylation and peracetic acid formation, consuming both pyruvate and O_2 (Figure 7). As a result, the relative concentrations of O_2 and pyruvate dictate the extent of buildup and the length of time for which LThDP is stable. Therefore, accumulation of LThDP over a long time period requires conditions where pyruvate is in excess to O_2, which is the case for previously reported CD and NMR experiments (15). Under these conditions, enzyme-catalyzed O_2 consumption deoxygenates the solution, resulting in a net accumulation of LThDP in the absence of O_2-dependent decarboxylation, reconciling the discrepancy in our understanding of DXP synthase mechanism.

Although the requirement of a small-molecule (e.g. D-GAP or O_2) to trigger efficient LThDP decarboxylation on DXP synthase is established, the mechanism by which this occurs is not fully elucidated. Several mechanistic studies of DXP synthase have revealed compelling evidence for D-GAP-dependent conformational changes (12, 16, 17). For example, a recent hydrogen-deuterium exchange mass spectrometry (HDX-MS) study showed that a donor substrate analog and D-GAP induce closed and open conformations of DXP synthase, respectively (12). It is conceivable that D-GAP binding induces a conformational change that destabilizes the LThDP intermediate, lowering the barrier for chemical decarboxylation of LThDP (12, 15, 16). Considering the proposal that 2-oxoacid decarboxylation is reversible on ThDP-

dependent enzymes (31-33), it is also possible that an equilibrium between LThDP and the C2α-carbanion/CO_2 is established on DXP synthase in a conformation that limits release of CO_2 from the enzyme. Subsequent binding of D-GAP could then drive the equilibrium triggering LThDP depletion and turnover. These mechanistic models cannot be distinguished by the tools used in this study. Although O_2 is structurally and chemically distinct from D-GAP, it appears to trigger depletion of LThDP with a comparable rate and imparts similar behavior to the CD_{313} signal of the LThDP species (Figure 12), suggesting a similar mechanism of LThDP decarboxylation is at play in the presence of these two triggers. Further studies are required to determine if O_2 can induce a conformational change on DXP synthase, toward understanding the mechanism by which O_2 and D-GAP induce LThDP decarboxylation and release of CO_2, and to determine if other natural triggers exist.

Moving forward, it is imperative to consider the O_2-dependent E-LThDP depletion in mechanistic studies of DXP synthase. First, we have shown that addition of O_2 to LThDP by sample mixing causes depletion of the CD_{313} signal, indicating that K_d determinations for donor substrates should be performed under anaerobic conditions to obtain the most accurate measurement. Second, it is imperative that studies aimed at identifying other inducers of LThDP decarboxylation or investigating the roles of active site residues in catalysis, are conducted under anaerobic conditions to avoid interfering side reactions or variable contributions of oxygenase activity on variants, both of which could confound results. Other challenges to investigating DXP synthase, such as structural studies, may also be resolved by working under anaerobic conditions.

In this study, we have uncovered a novel activity of DXP synthase, adding to the repertoire of chemistry that this unique enzyme can catalyze. Notably, we illustrate that O_2 is a structurally distinct trigger of LThDP decarboxylation which has important mechanistic and technical implications for the study of DXP synthase mechanism. These findings add a major piece to the mechanistic puzzle of DXP synthase and have enabled resolution of inconsistencies in the literature. Taken together, these results lay a foundation to gain a deeper understanding of the function of the unique mechanism of DXP synthase in the broader context of microbial metabolism.

Experimental Procedures

General methods

Unless otherwise noted, all reagents were obtained from commercial sources. Aerobic spectrophotometric analyses were performed on a Beckman DU800 UV/Visible spectrophotometer (Brea, CA, USA). Anaerobic spectrophotometric analyses were performed on a Varian Cary 50 UV/Visible spectrophotometer (Palo Alto, CA, USA). Anaerobic conditions were established either in a Baker-Ruskinn Invivo (Sanford, ME, USA) or a Coy Laboratory Products vinyl anaerobic chamber (Grass Lake, MI, USA). *E. coli* wild-type DXP synthase and *E. coli* MEP synthase (IspC) were overexpressed and purified as reported previously with minor modifications for the purification of anaerobic DXP synthase. (14, 34) To obtain anaerobic DXP synthase, the protein was overexpressed and purified as previously described (34) however the second dialysis was carried out in an anaerobic chamber in 50 mM 4-(2-hydroxyethyl)-1-piperazineethanesulfonic acid (HEPES), pH 8, 5% glycerol, 100 mM NaCl, 10 mM $MgCl_2$, and 1 mM ThDP at 0 ºC for 4 h. The protein was stored in liquid N_2 until use when it was transferred directly to an anaerobic chamber. Radioactivity measurements where made with a Beckman LS6500 scintillation counter (Brea, CA, USA). X-band (9 GHz) EPR measurements were made using a Varian E-112 spectrometer equipped with a TE_{102} cavity and interfaced to a PC using custom written software. Steady-state CD spectra were recorded on an Aviv 420 CD spectrometer (Lakewood, NJ, USA). Pre-steady state CD spectra were recorded on an Applied Photophysics Pi*-180 stopped-flow CD spectrometer (Leatherhead, Surrey, UK) with a 10-mm path length cuvette. NMR spectra were obtained on a Bruker Avance III 500 MHz NMR spectrometer (Billerica, MA, USA). Oxygen consumption was measured with the Oxytherm + respiration oxygen monitoring system from Hansatech Instruments Ltd (Norfolk, UK).

NMR detection of product formation by DXP synthase in the absence of D-GAP

To monitor reaction progress by NMR, DXP synthase (30 μM) was mixed with $^{13}C_3$-pyruvate (500 μM) in 50 mM HEPES-D_{18}, pH 8, 100 mM NaCl, 1 mM ThDP, 2 mM $MgCl_2$, 1 % glycerol, and 10% D_2O to initiate product formation. 1D ^{13}C spectra (500 MHz, 256 scans, 0.7 s/scan) were recorded over time at 25 °C. A control lacking enzyme was prepared in the same buffer and incubated at 25 °C for 4 h after which a spectrum was recorded. Spectra of $^{13}C_2$-acetate and ^{13}C-bicarbonate standards were obtained in the NMR buffer and with the same acquisition parameters.

$^{14}CO_2$ trapping under aerobic conditions in the absence of D-GAP

To measure $^{14}CO_2$ release from DXP synthase, the same general protocol from Eubanks and Poulter was conducted with some minor modifications (13). Briefly, reactions (250 μL) contained 30 μM DXP synthase and [1-^{14}C]-pyruvate diluted with cold pyruvate (0.18 μCi/μmol total pyruvate, 500 μM pyruvate total) in reaction buffer (50 mM HEPES, pH 8, 100 mM NaCl, 1 mM ThDP, 2 mM $MgCl_2$, and 1 % glycerol). Solutions were pre-incubated in the absence of DXP synthase at 0 °C for 5 min in the outer well of a trapping vial (glass vial, 4.5 cm height and 2.5 cm diameter, with 24/40 ground glass neck and a center well trap, 2 cm height and 1.5 cm diameter). The center well trap contained 500 μL of 1 M NaOH, and a 24/40 septum stopper was used to seal the trapping vial. Reactions were then initiated upon addition of DXP synthase to the outer well via syringe and incubated at 0 °C. At 0.5, 5, and 60 min, 250 μL of 12.5 % TCA in 1M HCl was added to the outer well of the trapping vial via syringe to quench the reaction and drive hydrated $^{14}CO_2$ out of solution (note each timepoint was a separate reaction). A negative control in which enzyme storage buffer (50 mM Tris, pH 8, 10 % glycerol, 100 mM NaCl, 10 mM $MgCl_2$, 1 mM ThDP) was added in place of enzyme was also prepared and "quenched" at 60 min. The quenched solutions were incubated at 25 °C for 2 h to trap the $^{14}CO_2$ released by DXP synthase. The entire contents of the acid quench solution and the NaOH trap solution were added to 10 mL of Hionic-Fluor scintillation fluid (Perkin Elmer), mixed by vortexing, and immediately counted (1-min counting time per sample). DPMs were determined from the measured CPMs using the counting efficiency determined from a standard curve of [1-^{14}C]-pyruvate in the acidic medium or [^{14}C]-bicarbonate in the basic medium. All reactions were carried out in triplicate. Because this quench and trapping protocol varied slightly from that of Eubanks and Poulter (13), a trapping control was conducted to confirm that >95 % of the $^{14}CO_2$ that is released from the enzyme is collected in our trap (Figure S5).

Lactate dehydrogenase detection of pyruvate consumption under aerobic conditions

For lactate dehydrogenase (LDH) detection of pyruvate consumption, reactions contained 30 μM DXP synthase and 500 μM pyruvate in reaction buffer (described above). These solutions were preincubated for 5 min at 0 °C in the absence of DXP synthase. Pyruvate consumption was initiated upon addition of DXP synthase or storage buffer for the no enzyme control. At 0.5, 5, and 60 min, a 60 μL aliquot of the reaction solution was boiled at 100 °C for 5 min to quench the reaction. Precipitated protein was pelleted by centrifugation. The pyruvate remaining in the quenched solution was then determined using LDH. Reactions (400 μL) containing 40 μL of the supernatant from the quenched reaction solution, 200 μM NADH, 32.5 mM KH_2PO_4, pH 7.4, and 0.75 U/mL yeast LDH were initiated upon addition of the pyruvate-containing solution and the absorbance at 340 nm (ε = 6220 M^{-1} cm^{-1}) was monitored at 37 °C for 15 min. The amount of pyruvate in each sample was calculated using the change in the initial and final absorbance. Corrections were made for non-enzymatic oxidation of NADH over the course of the LDH reaction. DXP synthase reactions were conducted in triplicate.

Detection of oxygen consumption

To determine if DXP synthase consumes O_2 in an enzyme- and substrate-dependent manner, DXP synthase concentration was varied (0- 30 μM) in the presence of 500 μM pyruvate, and pyruvate concentration was varied (0-500 μM) in the presence of 5 μM DXP synthase in reaction buffer (described above). Solutions were prepared in the absence of pyruvate, added to the electrode

chamber (calibrated fresh each day at 25 °C) and equilibrated at 25 °C for at least 4 min until the O_2 signal stabilized. O_2 consumption was initiated upon addition of pyruvate (25 µL regardless of the final [pyruvate]) by syringe, and the concentration of O_2 was monitored over time at 25 °C. O_2 consumption was monitored under each condition in triplicate.

Electron prarmagnetic reasonance detection of ThDP-enamine radical species

DXP synthase (32 mg/mL, 508 µM) in 0.4 ml of 50 mM HEPES (pH 8.0) containing 0.10 M NaCl, 1.0 mM ThDP, 10 mM $MgCl_2$ and 10 % glycerol was mixed with unlabeled pyruvate (10 mM), $^2H_3$-pyruvate (10 mM), or $^{13}C_3$-pyruvate (10 mM) at room temperature. Mixtures were immediately transferred into EPR tubes and flash-frozen in liquid nitrogen after a 30-40 s incubation at room temperature. During EPR measurements, the sample temperature was held at 77 K using an immersion finger dewar. Spectrometer parameters used to acquire the spectra are as follows: modulation amplitude: 5 G; microwave power, 10 µW; microwave frequency, 9.09 GHz; scan time, 2 min; time constant, 0.5 s; number of scans, 9. The field was calibrated using a standard sample of manganese doped in MgO (35). The concentration of active sites occupied by the ThDP radical species was calculated by comparing the double integral of the radical EPR spectrum with both Cu(II) and nitroxide standard sample spectra (23).

Colorimetric detection of DXP synthase-dependent peracetic acid formation

To determine if DXP synthase catalyzes the formation of peracetic acid as an intermediate in acetate formation, we utilized the previously described TNB assay (20). Samples were prepared in the reaction buffer described above with 75 µM TNB (synthesized and characterized according to the protocol in the SI) varying DXP synthase (0- 30 µM) in the presence of 500 µM pyruvate or varying pyruvate (0-500 µM) in the presence of 5 µM DXP synthase. After a 5-min preincubation at 25 ºC, peracetic acid formation was initiated upon addition of DXP synthase and the oxidation of TNB was monitored spectrophotometrically (λ_{max} = 412 nm, ε = 13,600 M^{-1} cm^{-1}) at 25 ºC over time. All reactions were carried out in triplicate.

$^{14}CO_2$ trapping under anaerobic conditions in the presence and absence of triggers

For the detection of $^{14}CO_2$ under anaerobic conditions the general method used for the aerobic $^{14}CO_2$ trapping assay was performed with some modifications. Before addition of the [1-^{14}C]-pyruvate, all solutions and the trapping vials (prepared with 500 µL of 1 M NaOH in the center well) were deoxygenated in an anaerobic chamber for 15 min at 30 ºC and then sealed with septa before removing from the chamber. [1-^{14}C]-Pyruvate was added to the reaction solution which was distributed to the outside wells of the trapping vials via syringe. One trapping vial was purged with 100 % O_2 for 10 min at 0 ºC before addition of the reaction solution. All trapping vials were then incubated at 0 ºC for 5 min. $^{14}CO_2$ release was initiated upon addition of DXP synthase, and the mixtures were incubated at 0 ºC for 1 h. The reactions were then quenched, trapped, and counted as described for aerobic conditions.

LDH detection of pyruvate consumption under anaerobic conditions

The same general method for LDH detection of pyruvate under aerobic conditions was repeated for a single 1-h timepoint under anaerobic conditions. Samples were prepared in the absence of DXP synthase, and both the reaction solutions and DXP synthase were purged in septa-capped Eppendorf tubes in the anaerobic chamber for 15 min at 30 ºC. All solutions were capped before removing from the chamber, and incubated at 0 ºC for 5 min. Pyruvate consumption was initiated upon addition of DXP synthase by syringe. After 1 h at 0 ºC, the samples were transferred to 100 ºC to quench the reactions. Precipitated DXP synthase was removed by centrifugation, and the pyruvate remaining in the supernatant was determined using the LDH assay as described above. Reactions were carried out in triplicate.

Steady state CD analysis of DXP synthase under anaerobic conditions

DXP synthase (30 µM) in 50 mM HEPES, pH 8, 100 mM NaCl, 1 mM $MgCl_2$, 1 mM BME, 0.2 mM ThDP (3 mL total) was deoxygenated in an anaerobic chamber for 30 min at 25 ºC. The sample was transferred to a septa-capped cuvette (Starna Cells, 1-Q-10-ST-S) which was closed before

removal from the chamber. A DXP synthase only scan was obtained from 450-280 nm at 4 ºC with a 1 nm step and 1.6 s averaging time. Pyruvate (7-401 μM) was titrated into the sample via syringe, and the CD spectrum after each addition of pyruvate was recorded as described above. The titration was carried out in triplicate. D-GAP (1 mM) or O_2 (via aeration of the sample by pipette) were added after the final pyruvate addition, and a spectrum obtained by the scan method described above. The normalized CD signal at 313 nm, indicative of LThDP on DXP synthase (15), was plotted against the concentration of pyruvate to obtain an apparent K_d^{pyr} and the plot was fit to a one-site specific binding curve in GraphPad Prism Version 6. All K_d determinations were performed in triplicate.

Steady state kinetic characterization of DXP formation under aerobic and anaerobic conditions

DXP formation was monitored using the previously described DXP synthase-IspC coupled assay with some modifications (14). Pyruvate concentration was varied (6.25-1000 μM) while holding D-GAP constant at 500 μM, or D-GAP concentration was varied (3.125- 1000 μM) while holding pyruvate constant at 1 mM with 100 nM DXP synthase, 2 μM IspC, and 200 μM NADPH in 100 mM HEPES, pH 8, 5 mM NaCl, 2.5 mM TCEP, 2 mM $MgCl_2$, and 1 mM ThDP. When D-GAP concentration was varied, samples were prepared without pyruvate and initiated with pyruvate. When pyruvate concentration was varied, samples were prepared without pyruvate or D-GAP, and enzymatic reactions were initiated with both substrates. For the anaerobic characterization, solutions were prepared from anaerobic stocks in an anaerobic chamber at 26 ºC (either prepared from solids in the chamber with deoxygenated water or solutions made anaerobic by incubation in the chamber for 15 min before sample preparation). Reaction solutions in septa-topped cuvettes (Starna cells, 9B-Q-10-GL14-S) and initiation solutions in septa-topped vials were sealed before removal from the chamber. Reactions where initiated upon addition of substrate via syringe as described above, and the solutions were mixed by tilting the cuvettes. Samples for the aerobic characterization were treated similarly but with constant exposure to room air. For both the aerobic and anaerobic characterizations, the depletion of NADPH (λ_{max} = 340 nm, ε = 6220 M^{-1} cm^{-1}) was monitored over time at 25 ºC following initiation of DXP formation. The rates of NADPH depletion were used to determine the initial rates of DXP formation. Plots of initial rate of DXP formation against [substrate] were fit to the Michaelis-Menten equation in GraphPad Prism Version 6. Reactions were performed in duplicate.

Pre-steady state CD characterization of LThDP formation under anaerobic conditions

For all pre-steady state experiments, the CD signal of LThDP at 313 nm was monitored at 6 ºC over time. All samples were prepared with anaerobic stocks (prepared from solids with deoxygenated water in an anaerobic chamber) in a portable glove box (Belart) under constant flow of 100 % N_2. Trace oxygen inside the glove box was removed with Anaero-Packs (Mitsubushi) and the O_2 level the chamber was monitored with Anaero-indicator tablets (Mitsubushi). Anaerobic conditions were established and maintained in the stopped flow CD using the anaerobic accessory and anaerobic operation protocol provided by Applied Photophysics. (36) To determine the rate of LThDP formation, DXP synthase (60 μM) in buffer A (50 mM HEPES, pH 8, 1 mM ThDP, 100 mM NaCl, 2 mM $MgCl_2$) was rapidly mixed with an equal volume of pyruvate (2 mM) in buffer A. The CD signal at 313 was monitored for 10 s at 6 ºC and the data from 7 repetitive shots were averaged. The data from 0.01 - 10 s were fit to a double exponential association model (Equation 1) using SigmaPlot version 10:

$$y(t) = y_0 + a^* (1-\exp(-k_1 t)) + b^*(1-\exp(-k_1' t))$$

Equation 1

where y_0 is the CD_{313} at t = 0, k_1 and k_1' represent the rate constants of the faster and slower phases of LThDP formation respectively, and a and b describe the maximum CD_{313} for the faster and slower phases, respectively. Error represents the error of the curve fit.

Pre-steady state CD characterization of decarboxylation rates in the presence and absence of triggers under anaerobic conditions

The effect of O_2 on the rates of LThDP decarboxylation and resynthesis in the presence and absence of D-GAP were determined by conducting the experiments under anaerobic conditions. For the rate of LThDP decarboxylation in the absence of triggers, LThDP was preformed in one syringe (60 μM DXP synthase and 1 mM pyruvate in buffer A described above) and mixed with an equal volume of buffer A in a second syringe under anaerobic conditions. The CD signal at 313 nm was monitored at 6 ºC for 5 s and the data from 7 repetitive shots were averaged. Determinations of the rates of LThDP decarboxylation in the presence of D-GAP and O_2 were conducted similarly except the second syringe contained either 1 mM D-GAP or oxygenated buffer A (prepared by bubbling 100% O_2 through 1 mL of buffer A for 1 h at 25 ºC), respectively. The data for LThDP decarboxylation were fit to a single exponential decay model (Equation 2) using SigmaPlot version 10:

$$y(t) = y_0 + a * \exp(-k_2 t)$$
Equation 2

where y_0 is the CD_{313} at t = 0, a describes the minimum CD_{313}, and k_2 represents the rate constant for LThDP decarboxylation. For the determination of LThDP decarboxylation rates, data points between 0.023 and 0.3 s were used in the (+) O_2 analysis and data points between 0.023 and 0.165 s were used in the (+) D-GAP analysis. Rates of LThDP resynthesis were determined using either the double exponential association model (Equation 1) for the (+) D-GAP experiment or a single association model (Equation 3) for the (+) O_2 experiment using SigmaPlot version 10:

$$y(t) = y_0 + a* (1-\exp(-k_{1r}t))$$
Equation 3

where y_0 is the CD_{313} at t = 0, a describes the maximum CD_{313}, and k_{1r} represents the rate constant for LThDP resynthesis. Data points between 0.358 and 5 s where used for the analysis of LThDP resynthesis in the presence of O_2 and data points between 0.2 and 5 s where used in the analysis of LThDP resynthesis in the presence of D-GAP. Error represents the error of the curve fit

Acknowledgments

The authors thank the Liz Calzada (Claypool Lab, JHMI), Risa Burr (Espenshade Lab, JHMI), and Erica Sinner (Townsend Lab, JHU) for kindly allowing access to instruments and advice on the study of oxygen consumption and work under anaerobic conditions. We are grateful to Melanie Johnston for her helpful discussion throughout the study, and her generous aid in establishing anaerobic techniques. We thank the JHU Biomolecular NMR Center for 600 MHz data collection. This work was supported by the National Institutes of Health grant to C.L.F.M R01 GM084998.

Conflict of Interest

The authors declare that they have no conflicts of interest with the contents of this article. The content is solely the responsibility of the authors and does not necessarily represent the official views of the National Institutes of Health.

Contributions

C.L.F.M. and A.A.D. conceived and designed the study and wrote the paper. A.A.D conducted and analyzed data for most of the experiments. N.S.N and A.A.D. performed the experiments and analyzed the data in Figures 11-12 and Table 3. A.M. performed the experiment and analyzed the data in Figure S1 and provided technical assistance and method development for the data in Figures 3B-C. N.S.N. and G.J.G. designed the experiment for Figure 6. G.J.G. conducted the experiment and analyzed the data for Figure 6. N.S.N., A.M., G.J.G, and F.J. contributed to the preparation of the manuscript. All authors reviewed the results and approved the final version of the manuscript.

References

1. Du, Q., Wang, H., and Xie, J. (2011) Thiamin (vitamin B1) biosynthesis and regulation: a rich source of antimicrobial drug targets?. *Int.J.Biol.Sci.* **7,** 41-52

2. Laber, B., Maurer, W., Scharf, S., Stepusin, K., and Schmidt, F.S. (1999) Vitamin B6 biosynthesis: formation of pyridoxine 5'-phosphate from 4-(phosphohydroxy)-L-threonine and 1-deoxy-D-xylulose-5-phosphate by PdxA and PdxJ protein. *FEBS Lett.* **449,** 45-48

3. Rodriguez-Concepcion, M. (2004) The MEP pathway: a new target for the development of herbicides, antibiotics and antimalarial drugs. *Curr.Pharm.Des.* **10,** 2391-2400

4. Sprenger, G.A., Schorken, U., Wiegert, T., Grolle, S., de Graaf, A.A., Taylor, S.V., Begley, T.P., Bringer-Meyer, S., and Sahm, H. (1997) Identification of a thiamin-dependent synthase in Escherichia coli required for the formation of the 1-deoxy-D-xylulose 5-phosphate precursor to isoprenoids, thiamin, and pyridoxol. *Proc.Natl.Acad.Sci.U.S.A.* **94,** 12857-12862

5. Bartee, D., Morris, F., Al-Khouja, A., and Freel Meyers, C.L. (2015) Hydroxybenzaldoximes Are D-GAP-Competitive Inhibitors of E. coli 1-Deoxy-D-Xylulose-5-Phosphate Synthase. *Chembiochem.* **16,** 1771-1781

6. Sanders, S., Vierling, R.J., Bartee, D., DeColli, A.A., Harrison, M.J., Aklinski, J.L., Koppisch, A.T., and Freel Meyers, C.L. (2017) Challenges and Hallmarks of Establishing Alkylacetylphosphonates as Probes of Bacterial 1-Deoxy-d-xylulose 5-Phosphate Synthase. *ACS Infect.Dis.* **3,** 467-478

7. Smith, J.M., Vierling, R.J., and Meyers, C.F. (2012) Selective inhibition of E. coli 1-deoxy-D-xylulose-5-phosphate synthase by acetylphosphonates(). *Medchemcomm.* **3,** 65-67

8. Smith, J.M., Warrington, N.V., Vierling, R.J., Kuhn, M.L., Anderson, W.F., Koppisch, A.T., and Freel Meyers, C.L. (2014) Targeting DXP synthase in human pathogens: enzyme inhibition and antimicrobial activity of butylacetylphosphonate. *J.Antibiot.(Tokyo).* **67,** 77-83

9. Schorken, U., and Sprenger, G.A. (1998) Thiamin-dependent enzymes as catalysts in chemoenzymatic syntheses. *Biochim.Biophys.Acta.* **1385,** 229-243

10. Xiang, S., Usunow, G., Lange, G., Busch, M., and Tong, L. (2007) Crystal structure of 1-deoxy-D-xylulose 5-phosphate synthase, a crucial enzyme for isoprenoids biosynthesis. *J.Biol.Chem.* **282,** 2676-2682

11. Morris, F., Vierling, R., Boucher, L., Bosch, J., and Freel Meyers, C.L. (2013) DXP synthase-catalyzed C-N bond formation: nitroso substrate specificity studies guide selective inhibitor design. *Chembiochem.* **14,** 1309-1315

12. Zhou, J., Yang, L., DeColli, A., Freel Meyers, C., Nemeria, N.S., and Jordan, F. (2017) Conformational dynamics of 1-deoxy-d-xylulose 5-phosphate synthase on ligand binding revealed by H/D exchange MS. *Proc.Natl.Acad.Sci.U.S.A.* **114,** 9355-9360

13. Eubanks, L.M., and Poulter, C.D. (2003) Rhodobacter capsulatus 1-deoxy-D-xylulose 5-phosphate synthase: steady-state kinetics and substrate binding. *Biochemistry.* **42,** 1140-1149

14. Brammer, L.A., Smith, J.M., Wade, H., and Meyers, C.F. (2011) 1-Deoxy-D-xylulose 5-phosphate synthase catalyzes a novel random sequential mechanism. *J.Biol.Chem.* **286,** 36522-36531

15. Patel, H., Nemeria, N.S., Brammer, L.A., Freel Meyers, C.L., and Jordan, F. (2012) Observation of thiamin-bound intermediates and microscopic rate constants for their interconversion on 1-deoxy-D-xylulose 5-phosphate synthase: 600-fold rate acceleration of pyruvate decarboxylation by D-glyceraldehyde-3-phosphate. *J.Am.Chem.Soc.* **134,** 18374-18379

16. Basta, L.A.B., Patel, H., Kakalis, L., Jordan, F., and Meyers, C.L.F. (2014) Defining critical residues for substrate binding to 1-deoxy-D-xylulose 5-phosphate synthase--active site substitutions stabilize the predecarboxylation intermediate C2alpha-lactylthiamin diphosphate. *FEBS J.* **281,** 2820-2837

17. Battistini, M.R., Shoji, C., Handa, S., Breydo, L., and Merkler, D.J. (2016) Mechanistic binding insights for 1-deoxy-D-Xylulose-5-Phosphate synthase, the enzyme catalyzing the first reaction of isoprenoid biosynthesis in the malaria-causing protists, Plasmodium falciparum and Plasmodium vivax. *Protein Expr.Purif.* **120,** 16-27

18. Brammer, L.A., and Meyers, C.F. (2009) Revealing substrate promiscuity of 1-deoxy-D-xylulose 5-phosphate synthase. *Org.Lett.* **11,** 4748-4751

19. Abell, L.M., and Schloss, J.V. (1991) Oxygenase side reactions of acetolactate synthase and other carbanion-forming enzymes. *Biochemistry.* **30,** 7883-7887

20. Schloss, J.V., Hixon, M.S., Chu, F., Chang, S., and Duggleby, R.G. (1996) Products formed in the oxygen-consuming reactions of acetolactate synthase and pyruvate decarboxylase. *Biochemistry and physiology of thiamin diphosphate enzymes:proceedings of the 4th international meeting on the function of thiamin diphosphate enzymes.* 580-585

21. Tse, M.T., and Schloss, J.V. (1993) The oxygenase reaction of acetolactate synthase. *Biochemistry.* **32,** 10398-10403

22. Mansoorabadi, S.O., Seravalli, J., Furdui, C., Krymov, V., Gerfen, G.J., Begley, T.P., Melnick, J., Ragsdale, S.W., and Reed, G.H. (2006) EPR spectroscopic and computational characterization of the hydroxyethylidene-thiamine pyrophosphate radical intermediate of pyruvate:ferredoxin oxidoreductase. *Biochemistry.* **45,** 7122-7131

23. Nemeria, N.S., Ambrus, A., Patel, H., Gerfen, G., Adam-Vizi, V., Tretter, L., Zhou, J., Wang, J., and Jordan, F. (2014) Human 2-oxoglutarate dehydrogenase complex E1 component forms a thiamin-derived radical by aerobic oxidation of the enamine intermediate. *J.Biol.Chem.* **289,** 29859-29873

24. Nemeria, N.S., Gerfen, G., Guevara, E., Nareddy, P.R., Szostak, M., and Jordan, F. (2017) The human Krebs cycle 2-oxoglutarate dehydrogenase complex creates an additional source of superoxide/hydrogen peroxide from 2-oxoadipate as alternative substrate. *Free Radic.Biol.Med.* **108,** 644-654

25. Nemeria, N.S., Gerfen, G., Nareddy, P.R., Yang, L., Zhang, X., Szostak, M., and Jordan, F. (2018) The mitochondrial 2-oxoadipate and 2-oxoglutarate dehydrogenase complexes share their E2 and E3 components for their function and both generate reactive oxygen species. *Free Radic.Biol.Med.* **115,** 136-145

26. Pierce, E., Mansoorabadi, S.O., Can, M., Reed, G.H., and Ragsdale, S.W. (2017) Properties of Intermediates in the Catalytic Cycle of Oxalate Oxidoreductase and Its Suicide Inactivation by Pyruvate. *Biochemistry.* **56,** 2824-2835

27. Tittmann, K., Wille, G., Golbik, R., Weidner, A., Ghisla, S., and Hubner, G. (2005) Radical phosphate transfer mechanism for the thiamin diphosphate- and FAD-dependent pyruvate oxidase from Lactobacillus plantarum. Kinetic coupling of intercofactor electron transfer with phosphate transfer to acetyl-thiamin diphosphate via a transient FAD semiquinone/hydroxyethyl-ThDP radical pair. *Biochemistry.* **44,** 13291-13303

28. Sung, M., Lee, H., Nam, K., Rexroth, S., Rögner, M., Kwon, J., and Yang, J. (2015) A simple method for decomposition of peracetic acid in a microalgal cultivation system. *Bioprocess Biosyst Eng.* **38,** 517-522

29. Putt, K.S., and Pugh, R.B. (2013) A high-throughput microtiter plate based method for the determination of peracetic acid and hydrogen peroxide. *PLoS One.* **8,** e79218

30. Bunik, V.I., Schloss, J.V., Pinto, J.T., Dudareva, N., and Cooper, A.J. (2011) A survey of oxidative paracatalytic reactions catalyzed by enzymes that generate carbanionic intermediates: implications for ROS production, cancer etiology, and neurodegenerative diseases. *Adv.Enzymol.Relat.Areas Mol.Biol.* **77,** 307-360

31. Gonzalez-James, O., and Singleton, D.A. (2010) Isotope Effect, Mechanism, and Origin of Catalysis in the Decarboxylation of Mandelylthiamin. *J.Am.Chem.Soc.* **132,** 6896-6897

32. Kluger, R. (2015) Decarboxylation, CO2 and the reversion problem. *Acc.Chem.Res.* **48,** 2843-2849

33. Mundle, S.O., Rathgeber, S., Lacrampe-Couloume, G., Sherwood Lollar, B., and Kluger, R. (2009) Internal return of carbon dioxide in decarboxylation: catalysis of separation and 12C/13C kinetic isotope effects. *J.Am.Chem.Soc.* **131,** 11638-11639

34. Nemeria, N.S., Shome, B., DeColli, A.A., Heflin, K., Begley, T.P., Meyers, C.F., and Jordan, F. (2016) Competence of Thiamin Diphosphate-Dependent Enzymes with 2'-Methoxythiamin Diphosphate Derived from Bacimethrin, a Naturally Occurring Thiamin Anti-vitamin. *Biochemistry.* **55,** 1135-1148

35. O Burghaus and M Rohrer and T Gotzinger and M Plato and, K Mobius (1992) A novel high-field/high-frequency EPR and ENDOR spectrometer operating at 3 mm wavelength. *Measurement Science and Technology.* **3,** 765

36. Applied Photophysics (2012) User Manual
SX20 Stopped Flow Spectrometer

Footnotes

This work was supported by the National Institutes of Health grant to C.L.F.M R01 GM084998. The authors declare that they have no conflicts of interest with the contents of this article. The content is solely the responsibility of the authors and does not necessarily represent the official views of the National Institutes of Health.

Abbreviations

DXP, 1-deoxy-D-xylulose 5-phosphate; ThDP, thiamin diphosphate; D-GAP, D-glyceraldehyde 3-phosphate; LThDP, C2α-lactylThDP; CD, circular dichroism; DCPIP, 2,6-dichlorophenolindophenol; HEThDP, hydroxyethylThDP; ThDP-enamine radical, C2-(α-hydroxy)-ethylideneThDP radical cation; DXPS, DXP synthase; EPR, electron paramagnetic resonance, TNB, thionitrobenzoate; HDX-MS, hydrogen-deuterium exchange mass spectrometry, HEPES, 4-(2-hydroxyethyl)-1-piperazineethanesulfonic acid; LDH, lactate dehydrogenase.

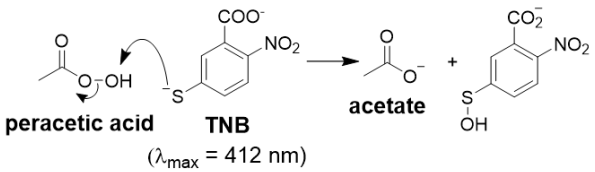

[DXP synthase] (μM)	Rate of O_2 consumption (μM/min)	Rate of peracetate formation (μM/min)
0	1.3 ± 0.2	-0.004 ± 0.004
0.5	5.1 ± 0.6	5.6 ± 0.3
1	8.9 ± 0.9	9.5 ± 0.1
5	38 ± 2	31 ± 1
5, (-) pyruvate	0.77 ± 0.08	0.000 ± 0.001

Table 1. Rates of peracetic acid formation in the presence of varying concentrations of DXP synthase and 500 μM pyruvate at 25 ºC are comparable to rates of O_2 consumption under the same conditions supporting Path A (Figure 4) as the major route for oxidative decarboxylation of pyruvate. Error represents standard error, n = 3

Condition	$K_m^{D\text{-}GAP}$ (μM)	$K_m^{pyruvate}$ (μM)	$K_D^{pyruvate}$ (μM)	k_{cat} (min^{-1})
Aerobic	8 ± 3	14.7 ± 0.2	89 ± 3[a]	84 ± 2
Anaerobic	6 ± 2	20.77 ± 0.01	45 ± 2	92 ± 5

[a] Patel *et al.* (15)

Table 2. Summary of steady state kinetic and binding parameters determined for DXP synthase under anaerobic conditions at 25 °C. Error represents standard deviation, n = 2.

	LThDP formation (s^{-1})	LThDP decarboxylation (s^{-1})			LThDP resynthesis (s^{-1})		
Condition	**(-) GAP**	**(-) GAP**	**(+) GAP**	**(+) O_2**	**(-) GAP**	**(+) GAP**	**(+) O_2**
Aerobic[a]	k_1 = 1.39 ± 0.05 (k_1' = 0.16 ± 0.02)	k_2 = 0.07 ± 0.001	k_2 = 42 ± 1	ND[b]	ND[c]	k_{1r} = 0.68 ± 0.01	ND[b]
Anaerobic	k_1 = 1.64 ± 0.21 (k_1' = 0.36 ± 0.03)	ND[c]	k_2 = 50.3 ± 7.8	k_2 = 62.0 ± 8.9	k_{1r} = 1.04 ± 0.11	k_{1r} = 1.67 ± 0.37 (k_{1r}' = 0.32 ± 0.25)	k_{1r} = 0.53 ± 0.02

[a] Basta *et al.* (16) [b] All experiments performed in the presence of O_2 [c] Rate could not be accurately determined

Table 3. Summary of pre-steady state kinetic parameters of DXP synthase in the presence and absence of D-GAP under aerobic and anaerobic conditions.

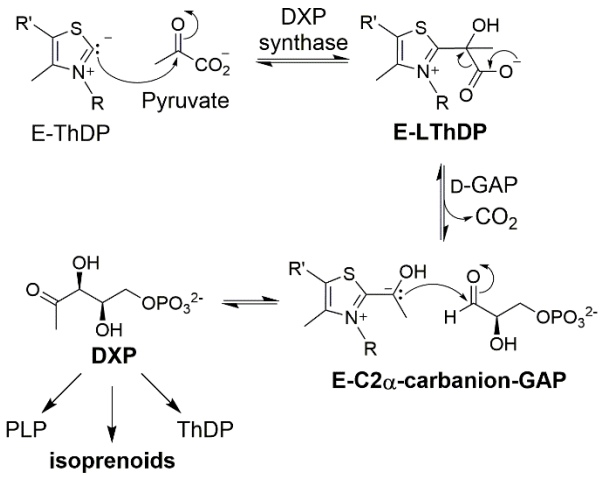

Figure 1. DXP synthase catalyzes the formation of the essential branch point metabolite, DXP, from pyruvate and D-GAP.

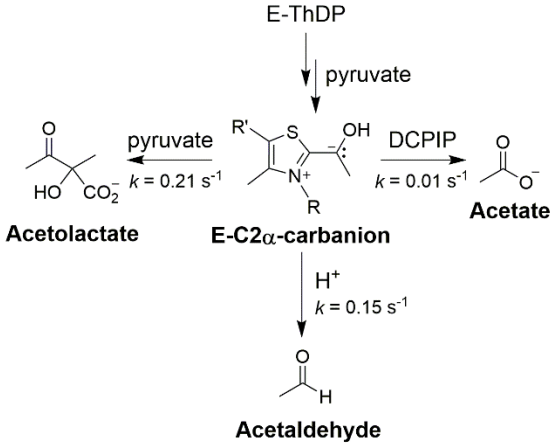

Figure 2. Reactions of the C2α-carbanion intermediate are exceedingly slow in the absence of D-GAP at 37 ºC (15) indicating the C2α-carbanion intermediate does not build up on DXP synthase.

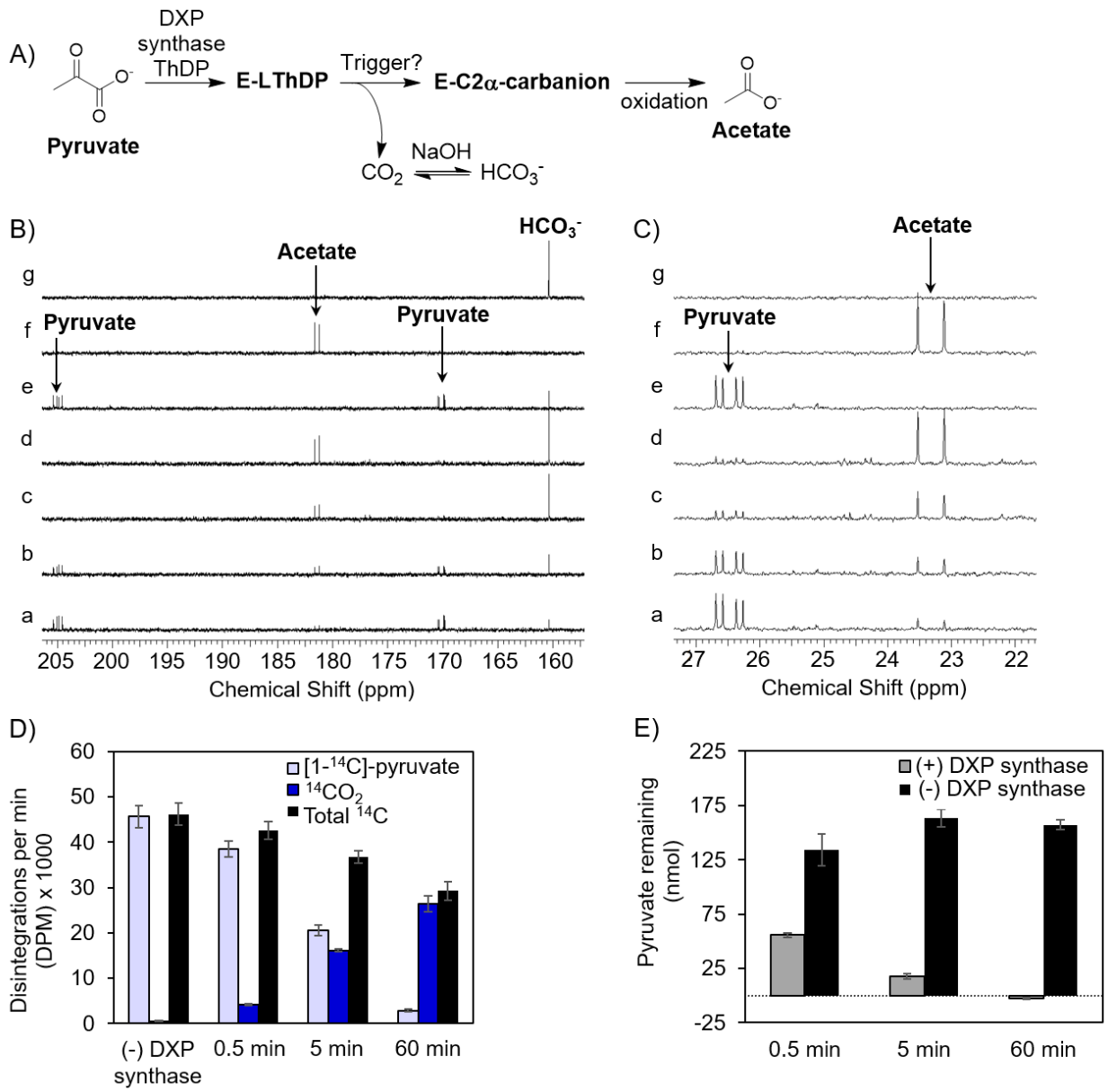

Figure 3. A) DXP synthase-mediated pyruvate consumption to form acetate and HCO_3^-. **B)** and **C**) ^{13}C NMR time course of the reaction of 30 µM DXP synthase with 3 mM $^{13}C_3$-pyruvate at 25 ºC in the absence of D-GAP (a. 3 min, b. 1 h, c. 4 h). At 4 h, $^{13}C_2$-acetate and ^{13}C-bicarbonate (3 mM) were added to the reaction mixture (d). Pyruvate is not consumed in the absence of DXP synthase (e). Spectra were acquired of $^{13}C_2$-acetate and ^{13}C-bicarbonate (f and g). **D**) $^{14}CO_2$ release is detected in a reaction containing 30 µM DXP synthase and [1-^{14}C]-pyruvate (0.18 µCi/µmol pyruvate, 500 µM total pyruvate) at 0 ºC. **E**) Pyruvate (500 µM) consumption in the presence of 30 µM (7.2 nmol) DXP synthase at 0 ºC is detected by the LDH assay. Error bars represent standard error, n = 3

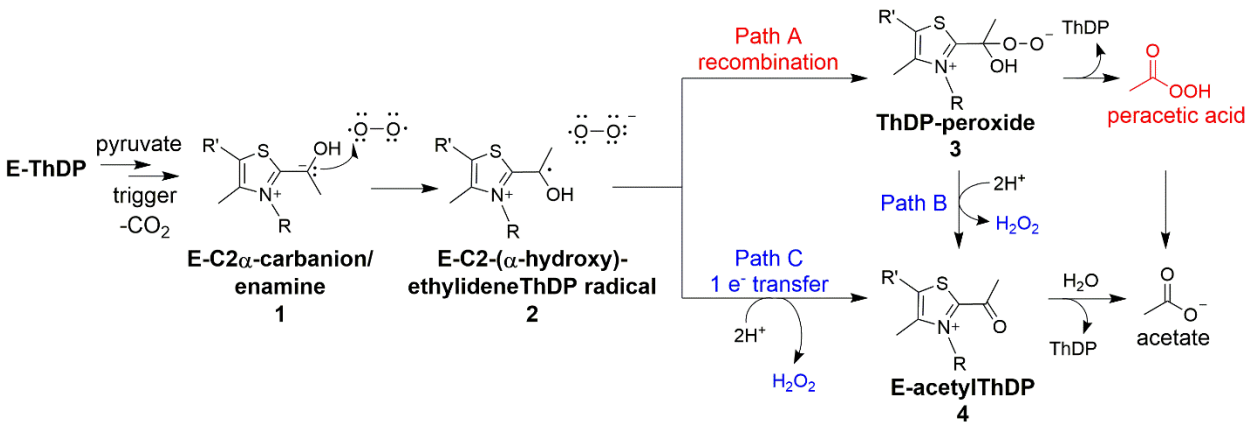

Figure 4. Possible routes for acetate formation via DXP synthase-catalyzed oxidative decarboxylation of pyruvate.

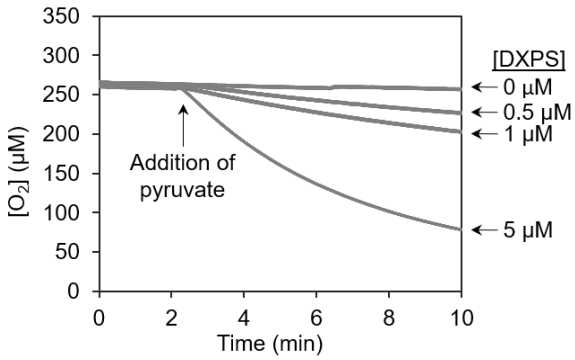

Figure 5. DXP synthase-dependent O_2 consumption is observed at 25 ºC in the presence of varying DXP synthase (DXPS) concentrations and pyruvate (500 μM). Representative data shown (n = 3).

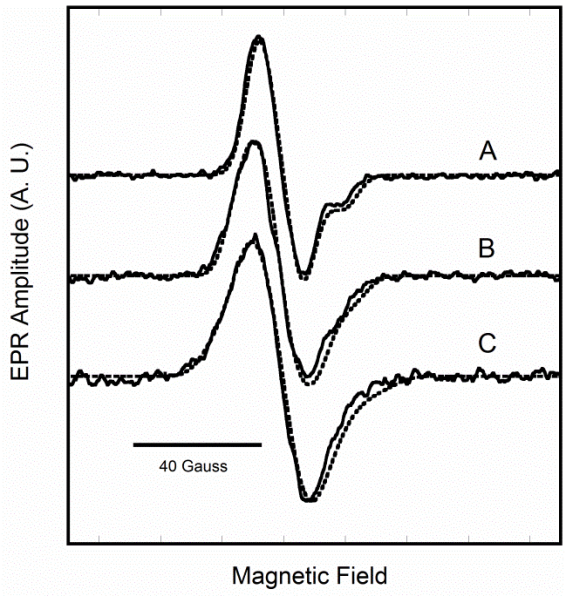

Figure 6. X-band (9 GHz) CW-EPR spectra of the radical species generated by DXP synthase (508 μM) in the presence of 10 mM $^{2}H_3$-pyruvate (**A**), unlabeled pyruvate (**B**), or $^{13}C_3$-pyruvate (**C**). Solid lines represent experimental data and dashed lines are simulations generated using parameters given in Table S1 which are consistent with the radical structure **2**, Figure 4. Simulation details are provided in the supplementary information.

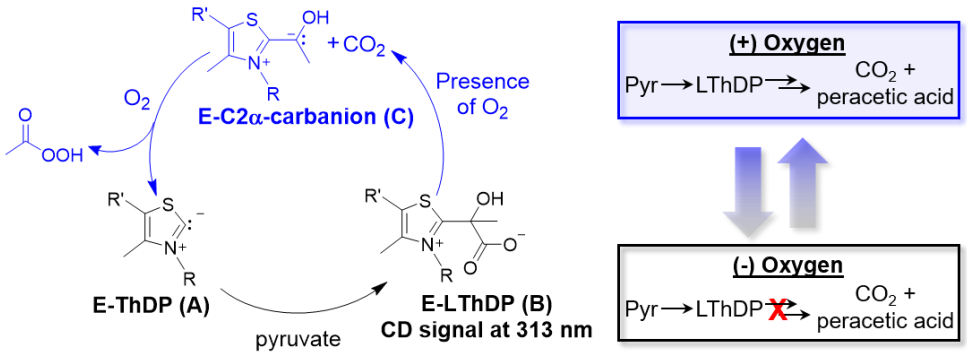

Figure 7. Proposed model for oxidative decarboxylation of pyruvate illustrating the roles of O_2 as 1) a trigger for CO_2 release, and 2) an acceptor substrate in peracetic acid formation. This catalytic cycle results in depletion of O_2, pyruvate, and LThDP, and the amount of LThDP accumulation and/or peracetic acid formation is expected to depend on the relative levels of O_2 and pyruvate in a given sample.

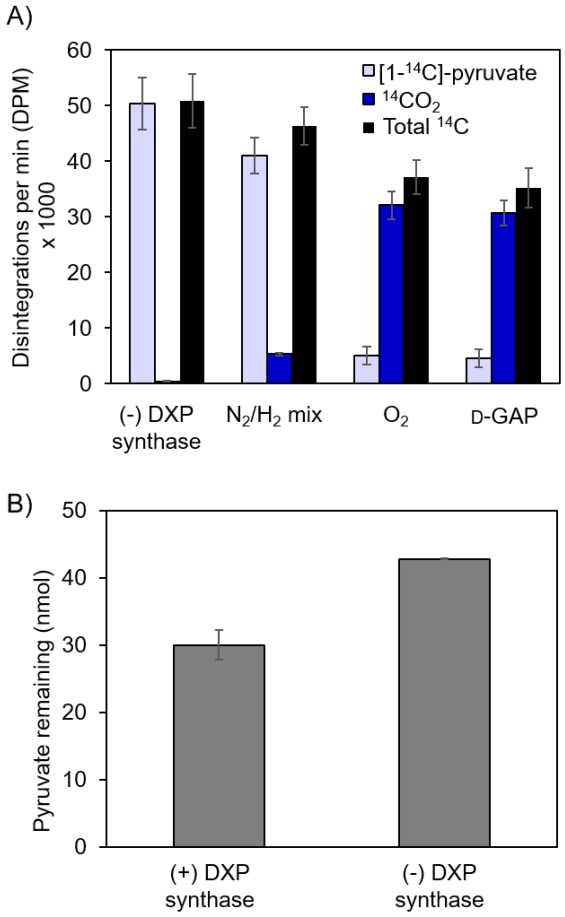

Figure 8. A) Detection of $^{14}CO_2$ release following incubation of DXP synthase **(**30 µM) and [1-^{14}C]-pyruvate (0.18 µCi/µmol pyruvate, 500 µM pyruvate total) for 60 min at 0 ºC under anaerobic conditions (90 % N_2/ 10 % H_2), in the presence or absence of O_2 (septa-capped trapping vial purged with 100 % O_2 for 10 min prior to addition of the reaction solution) or D-GAP (1 mM). **B**) LDH detection of pyruvate remaining in solution after a 60 min incubation of pyruvate (500 µM, 32.5 nmol) in the presence or absence of DXP synthase (30 µM, 1.95 nmol) at 0 ºC under anaerobic conditions. Error bars represent standard error, n = 3

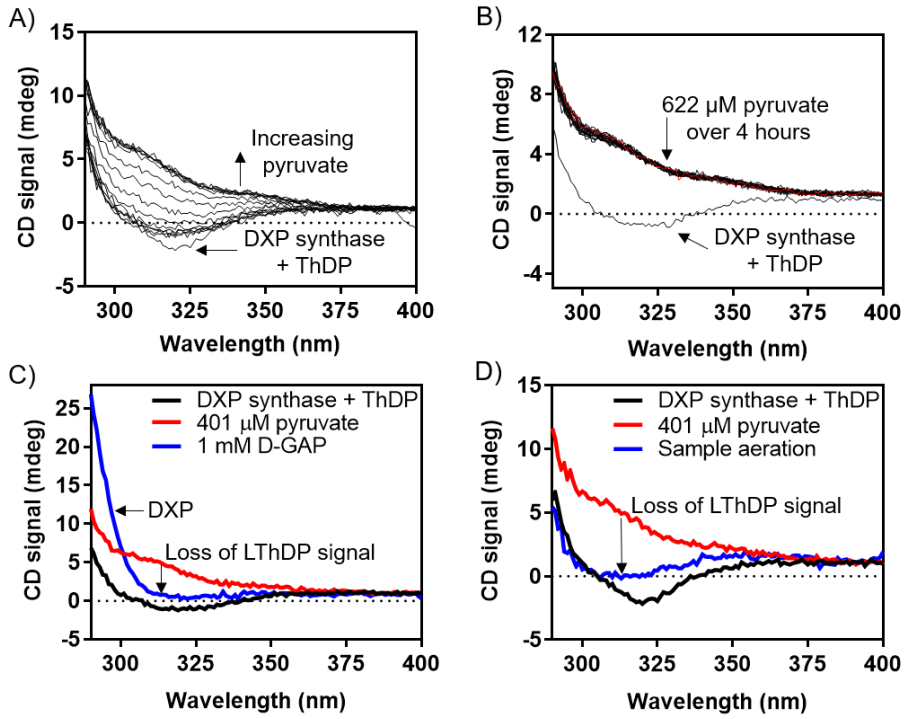

Figure 9. A) Titration of pyruvate onto DXP synthase (30 µM) at 4 ºC under anaerobic conditions reveals an apparent $K_d^{pyruvate}$ of 45 ± 2 µM (Error represents standard error, n = 3). A representative titration is shown). **B**) The CD signal at 313 nm (characteristic of LThDP) is stable on DXP synthase under anaerobic conditions for > 4 h at 4 ºC. Addition of D-GAP (**C**) or aeration (**D**) of a sample of preformed LThDP results in depletion of the LThDP CD signal at 313 nm.

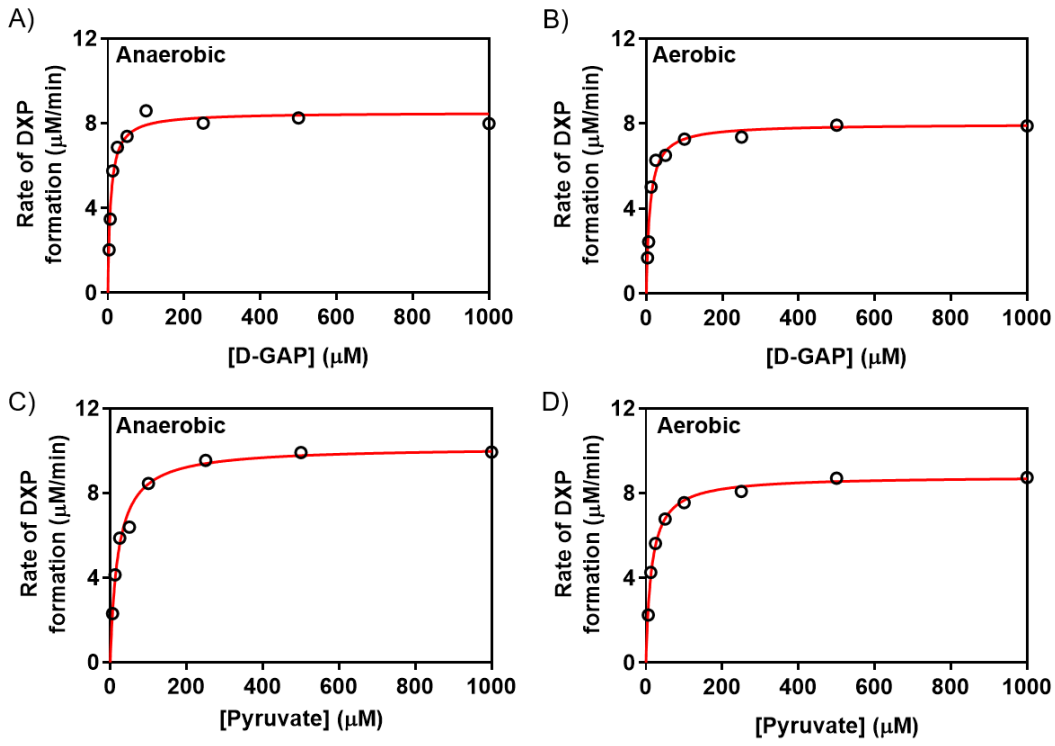

Figure 10. Representative Michaelis-Menten curves for DXP synthase determined with the IspC-coupled assay at 25 ºC varying D-GAP under anaerobic (**A**) or aerobic conditions (**B**) and varying pyruvate under anaerobic (**C**) or aerobic conditions (**D**).

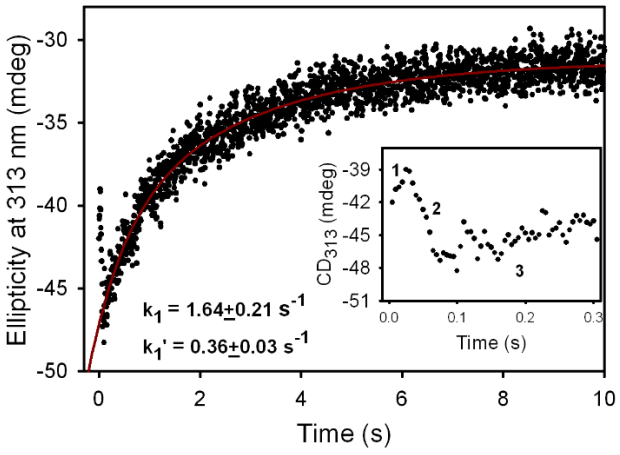

Figure 11. Pre-steady state formation of LThDP on DXP synthase (30 μM) in the presence of 1 mM pyruvate under anaerobic conditions at 6 ºC. A lag (region 1) and a decrease (region 2) in the CD signal at 313 nm are observed upon addition of pyruvate to the DXP synthase-ThDP complex prior to LThDP formation (region 3). Data points are an average of the CD signal over time from 7 repetitive shots. Error is calculated from the fit of the averaged data to a double exponential rise to a maximum (see Equation 1 in Materials and Methods)

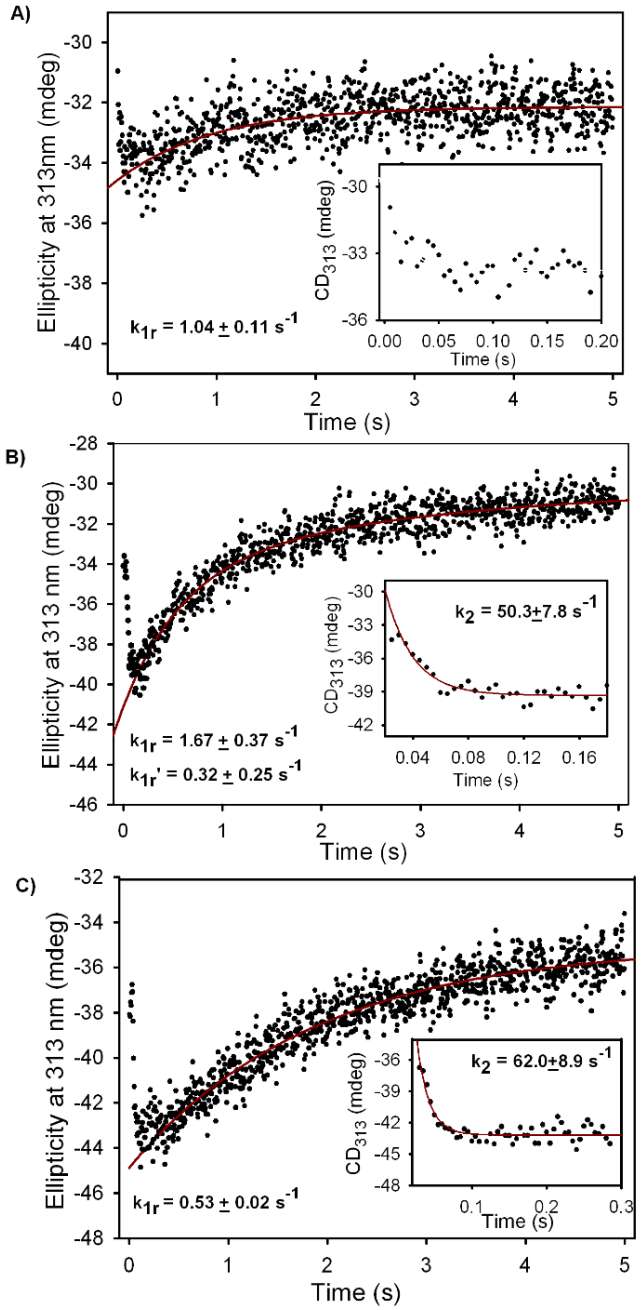

Figure 12. Pre-steady state decarboxylation of LThDP at 6 ºC upon addition of anaerobic buffer (**A**), an anaerobic solution of D-GAP (**B**), or O_2 saturated buffer (**C**) to preformed LThDP under anaerobic conditions. Insets show up to the first 300 ms of the full time course to illustrate the lags in the CD signal at 313 nm before and after LThDP decarboxylation. Data points are an average of the CD signal over time from 7 repetitive shots. Error is calculated from the fit of the averaged data to the appropriate equation (see Materials and Methods)

Oxidative decarboxylation of pyruvate by 1-deoxy-D-xylulose 5-phosphate synthase, a central metabolic enzyme in bacteria

Alicia A. DeColli, Natasha S. Nemeria, Ananya Majumdar, Gary J. Gerfen, Frank Jordan and Caren L. Freel Meyers

J. Biol. Chem. published online May 21, 2018
